

# Chiral dynamics of the $\Lambda(1520)$ in coupled channels tested in the $K^- p \rightarrow \pi\pi\Lambda$ reaction

Sourav Sarkar<sup>1</sup>, L. Roca, E. Oset, V. K. Magas and M. J. Vicente Vacas

*Departamento de Física Teórica and IFIC, Centro Mixto Universidad de Valencia-CSIC,  
Investigación de Paterna, Aptdo. 22085, 46071 Valencia, Spain*

**Abstract.** The  $\Lambda(1520)$  resonance is generated dynamically in a unitary coupled channel framework with the  $\pi\Sigma^*$  and  $K\Xi^*$  channels in  $s$ -wave and  $\pi\Sigma$  and  $\bar{K}N$  channels in  $d$ -wave. The dynamics of this resonance close to and above threshold is then tested through the reactions  $K^- p \rightarrow \pi\pi\Lambda$  and a good agreement with the experimentally measured cross section is observed.

**Keywords:** dynamical generation, Bethe-Salpeter equation

**PACS:** 11.10.St, 11.80.Gw, 13.60.Rj, 13.75.Jz

Application of unitary techniques to the lowest order chiral Lagrangian involving the octet of pseudoscalar mesons and the decuplet of baryons have led to the successful generation of a number of  $\frac{3}{2}^-$  resonances [1, 2, 3]. From the information of the pole positions and couplings to the channels involved of these resonances could be associated to the  $N^*(1520)$ ,  $\Delta(1700)$ ,  $\Lambda(1520)$ ,  $\Sigma(1670)$ ,  $\Sigma(1940)$ ,  $\Xi(1820)$  tabulated by the Particle Data Group (PDG). The  $\Lambda(1520)$ , in particular, is generated dynamically in the coupled channel interaction of the  $\pi\Sigma^*$  and  $K\Xi^*$  channels and appears at a higher energy than the nominal one and with a width much larger than the physical width [2]. Since the width of the  $\Lambda(1520)$  resonance comes basically from the decay into the  $\bar{K}N$  and  $\pi\Sigma(1193)$ , the introduction of these channels is mandatory to reproduce the shape of the  $\Lambda(1520)$  resonance. The novelty with respect to the other channels already accounted for in [2], which couple in  $s$ -wave, is that these new channels couple in  $d$ -waves. These channels are introduced phenomenologically using for the vertices  $\bar{K}N \rightarrow \bar{K}N$ ,  $\bar{K}N \rightarrow \pi\Sigma$  and  $\pi\Sigma \rightarrow \pi\Sigma$  effective transition potentials which are proportional to the incoming and outgoing momentum squared. Denoting  $\pi\Sigma^*$ ,  $K\Xi^*$ ,  $\bar{K}N$  and  $\pi\Sigma$  channels by 1, 2, 3 and 4 respectively, the matrix containing the tree level amplitudes is written as [4, 5]

$$V = \begin{pmatrix} C_{11}(k_1^0 + k_1^0) & C_{12}(k_1^0 + k_2^0) & \gamma_{13} q_3^2 & \gamma_{14} q_4^2 \\ C_{21}(k_2^0 + k_1^0) & C_{22}(k_2^0 + k_2^0) & 0 & 0 \\ \gamma_{13} q_3^2 & 0 & \gamma_{33} q_3^4 & \gamma_{34} q_3^2 q_4^2 \\ \gamma_{14} q_4^2 & 0 & \gamma_{34} q_3^2 q_4^2 & \gamma_{44} q_4^4 \end{pmatrix}, \quad (1)$$

where  $q_i = \frac{1}{2\sqrt{s}} \sqrt{[s - (M_i + m_i)^2][s - (M_i - m_i)^2]}$ ,  $k_i^0 = \frac{s - M_i^2 + m_i^2}{2\sqrt{s}}$  and  $M_i(m_i)$  is the baryon(meson) mass. The coefficients  $C_{ij}$  are  $C_{11} = \frac{-1}{f^2}$ ,  $C_{21} = C_{12} = \frac{\sqrt{6}}{4f^2}$  and  $C_{22} = \frac{-3}{4f^2}$ ,

<sup>1</sup> Present address: Variable Energy Cyclotron Centre, 1/AF, Bidhannagar, Kolkata-700091, India

where  $f$  is  $1.15f_\pi$ , with  $f_\pi$  ( $= 93$  MeV) the pion decay constant, which is taken as an average between  $f_\pi$  and  $f_K$ . The elements  $V_{11}$ ,  $V_{12}$ ,  $V_{21}$ ,  $V_{22}$  come from the lowest order chiral Lagrangian involving the decuplet of baryons and the octet of pseudoscalar mesons [2, 1]. We neglect the elements  $V_{23}$  and  $V_{24}$  which involve the tree level interaction of the  $K\Xi^*$  channel to the  $d$ -wave channels because the  $K\Xi^*$  threshold is far away from the  $\Lambda(1520)$ . We also emphasize that the consideration of the width of the  $\Sigma^*$  resonance in the loop function  $G$  is crucial in order to account properly for the  $\pi\Sigma^*$  channel since the threshold lies in the  $\Lambda(1520)$  region. This is achieved through the convolution of the  $\pi\Sigma^*$  loop function with the spectral distribution considering the  $\Sigma^*$  width.

In the model described so far we have as unknown parameters  $\gamma_{13}$ ,  $\gamma_{14}$ ,  $\gamma_{33}$ ,  $\gamma_{34}$ ,  $\gamma_{44}$  in the  $V$  matrix. Apart from these, there is also the freedom in the value of the subtraction constants in the loop functions. We will consider one subtraction constant for the  $s$ -wave channels ( $a_0$ ) and one for the  $d$ -wave ones ( $a_2$ ). Despite the apparent large number of free parameters in the  $V$  matrix, it is worth emphasizing that the largest matrix elements are  $V_{11}$ ,  $V_{12}$  and  $V_{22}$  [2] which come from a chiral Lagrangian without any free parameters. Due to the  $d$ -wave behavior the other ones are much smaller, as expected, as we see from the values of the parameters  $\gamma$  given below. In order to obtain these parameters we fit the partial wave amplitudes obtained by using the  $V$  matrix given above as the kernel in the Bethe-Salpeter equation to the experimental results on the  $\bar{K}N$  and  $\pi\Sigma$  scattering amplitudes in  $d$ -wave and  $I = 0$ . We use experimental data from [6, 7] where  $\bar{K}N \rightarrow \bar{K}N$  and  $\bar{K}N \rightarrow \pi\Sigma$  amplitudes are provided from partial wave analysis. From the fit we obtain the subtraction constants  $a_0 = -1.8$  for the  $s$ -wave channels and  $a_2 = -8.1$  for the  $d$ -wave channels. The unknown constants in the  $V$  matrix are given by  $\gamma_{13} = 0.98$  and  $\gamma_{14} = 1.1$  in units of  $10^{-7} \text{ MeV}^{-3}$  and  $\gamma_{33} = -1.7$ ,  $\gamma_{44} = -0.7$  and  $\gamma_{34} = -1.1$  in units of  $10^{-12} \text{ MeV}^{-5}$ .

From the imaginary part of the amplitudes it is straightforward to obtain the couplings of the  $\Lambda(1520)$  to the different channels. Up to a global sign of one of the couplings (we choose  $g_1$  to be positive), the couplings we obtain are shown in Table 1. We can see

**TABLE 1.** Couplings of the  $\Lambda(1520)$  resonance to the different channels

$g_1$	$g_2$	$g_3$	$g_4$
0.91	-0.29	-0.54	-0.45

from the values that the  $\Lambda(1520)$  resonance couples most strongly to the  $\pi\Sigma^*$  channel. The fact that we are able to predict the value of this coupling is a non trivial consequence of the unitarization procedure that we employ.

The prediction of the amplitudes involving  $\pi\Sigma^*$  channels can be checked in particular reactions where this channel could play an important role. We evaluate the cross section for  $K^- p \rightarrow \pi\pi\Lambda$  in the lines of [4] but using the new coupled channel formalism. The mechanisms and the expressions for the amplitudes and the cross sections can be found in [4] where, apart from the coupled channel unitarized amplitude, other mechanisms of relevance above the  $\Lambda(1520)$  peak were also included. In fig. 1 we show our results for  $K^- p \rightarrow \pi^0\pi^0\Lambda$  and  $K^- p \rightarrow \pi^+\pi^-\Lambda$  cross section on the left and right panels along with experimental data from refs. [8] and [9] respectively. The dashed line in the left figure

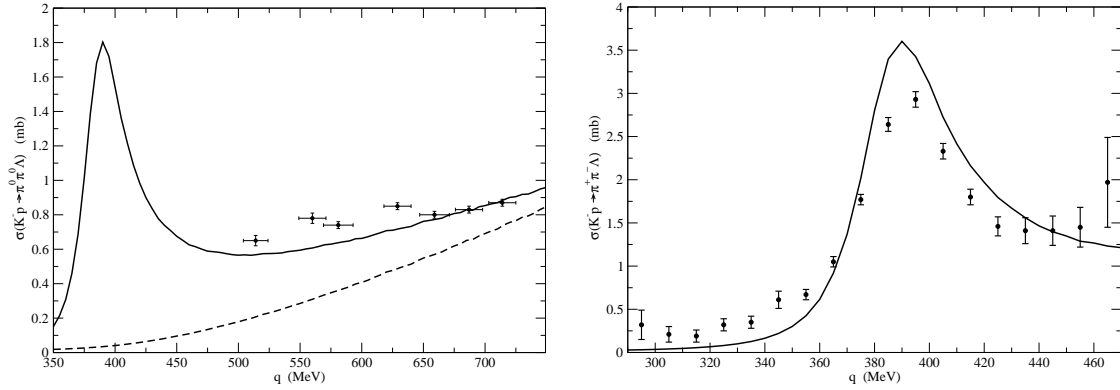


**FIGURE 1.** Result for the  $K^-p \rightarrow \pi^0\pi^0\Lambda$  (left) and  $K^-p \rightarrow \pi^+\pi^-\Lambda$  (right) cross section.

represents the contribution from mechanisms other than the unitarized coupled channels, and the solid line gives the coherent sum of all the processes. These cross sections depend essentially on the amplitude  $T_{\bar{K}N \rightarrow \pi\Sigma^*}$  which we obtain from our analysis.

In conclusion, we have done a unitary coupled channel analysis of the  $\Lambda(1520)$  resonance using the  $\pi\Sigma^*$ ,  $K\Xi^*$  channels in  $s$ -wave and the  $\bar{K}N$  and  $\pi\Sigma$  channels in  $d$ -wave. Our predictions of the amplitudes and couplings of the  $\Lambda(1520)$  to the different channels were tested in the  $K^-p \rightarrow \Lambda\pi^0\pi^0$  and  $K^-p \rightarrow \Lambda\pi^+\pi^-$  reactions for which the magnitude of the absolute cross section agrees fairly well with experimental data at energies close to and slightly above the  $\Lambda(1520)$  region.

## ACKNOWLEDGMENTS

This work is partly supported by DGICYT contract number BFM2003-00856, and the E.U. EURIDICE network contract no. HPRN-CT-2002-00311. This research is part of the EU Integrated Infrastructure Initiative Hadron Physics Project under contract number RII3-CT-2004-506078.

## REFERENCES

1. E. E. Kolomeitsev and M. F. M. Lutz, Phys. Lett. B **585** (2004) 243; M. F. M. Lutz and E. E. Kolomeitsev, Nucl. Phys. A **755** (2005) 29.
2. S. Sarkar, E. Oset and M. J. Vicente Vacas, Nucl. Phys. A **750** (2005) 294; Eur. Phys. J. A **24** (2005) 287.
3. M. J. Vicente Vacas, E. Oset and S. Sarkar, Int. J. Mod. Phys. A **20** (2005) 1826; S. Sarkar, E. Oset and M. J. Vicente Vacas, Nucl. Phys. A **755** (2005) 665 ; E. Oset, S. Sarkar, M. J. Vicente Vacas, A. Ramos, D. Jido, J. A. Oller and U. G. Meissner, Int. J. Mod. Phys. A **20** (2005) 1619; S. Sarkar, L. Roca, E. Oset, V. K. Magas and M. J. V. Vacas, arXiv:nucl-th/0511062.
4. S. Sarkar, E. Oset and M. J. Vicente Vacas, Phys. Rev. C **72** (2005) 015206.
5. L. Roca, S. Sarkar, V. K. Magas and E. Oset, (in preparation).
6. G. P. Gopal *et al.*, Nucl. Phys. B **119** (1977) 362.
7. M. Alston-Garnjost *et al.*, Phys. Rev. D **18** (1978) 182.
8. S. Prakhov *et al.*, Phys. Rev. C **69** (2004) 042202.
9. T. S. Mast *et al.*, Phys. Rev. D **7** (1973) 5.